Article

Dimensionality Alteration and Intra- versus Inter-SBU Void Encapsulation in Zinc Phosphate Frameworks[†]

Aijaz A. Dar,[‡] Gulzar A. Bhat, and Ramaswamy Murugavel*

Department of Chemistry, Indian Institute of Technology Bombay, Powai, Mumbai 400076, India

Ⓢ *Supporting Information*

ABSTRACT: 4,4′-Bipyridine-*N*-oxide (BIPYMO, **1**), a less commonly employed coordination polymer linker, has been used as a ditopic spacer to bridge double-four-ring (D4R) zinc phosphate clusters to form novel framework coordination polymers. Zinc phosphate framework compounds $[Zn_4(X\text{-}dipp)_4(BIPYMO)_2]_n \cdot 2MeOH$ [X = H (**2**), Cl (**3**), Br (**4**), I (**5**); dipp = 2,6-diisopropylphenyl phosphate] have been obtained by treating a methanol solution of zinc acetate with X-dippH$_2$ and BIPYMO (in a 1:1:1 molar ratio) at ambient conditions. Framework phosphates **2−5** can also be obtained by treating the preformed D4R cubanes $[Zn(X\text{-}dipp)\text{-}(DMSO)]_4$ with required quantities of BIPYMO in methanol.

Single-crystal X-ray diffraction studies reveal that these framework solids are two-dimensional (2D) networks as opposed to the diamondoid networks obtained when the parent unoxidized 4,4′-bipyridine is used as the linker (*Inorg. Chem.* **2014**, *53*, 8959). The two types of voids (viz., smaller intra-D4R and larger inter-D4R) present in these framework solids can be utilized for different types of encapsulation processes. For example, the in situ generated 2D framework **2** encapsulates fluoride ions accompanied by a change in the dimensionality of the framework to yield $\{[(nC_4H_9)_4N][F@(Zn_4(dipp)_4(BIPYMO)_2)]\}_n$ (**6**). The three-dimensional framework **6** represents the first structurally characterized example of a fluoride-ion-encapsulated polymeric coordination compound or a metal−organic framework. The possibility of utilizing inter-D4R voids as hosts for small organic molecules has been explored by treating in situ generated **2** with a series of organic molecules of appropriate size. Framework **2** has been found to be a selective host for benzil and not for other structurally similar molecules such as benzoquinone, benzidine, anthracene, naphthalene, α-pyridoin, etc. The benzil-occluded isolated framework [benzil@{Zn$_4$(dipp)$_4$(BIPYMO)$_2$}]$_n$ (**7**) has been isolated as single crystals, and its crystal structure determination revealed the binding of benzil molecules to the framework through strong π−π interactions.
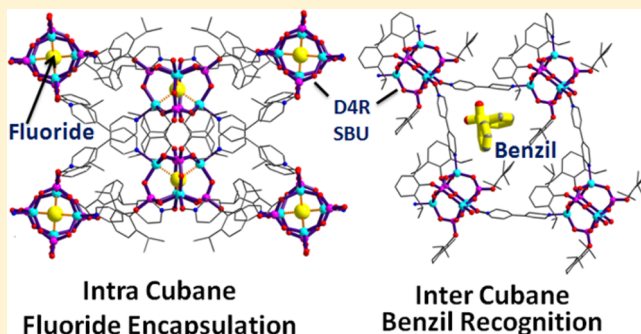
1. INTRODUCTION

Porous materials such as zeolites, metal−organic frameworks (MOFs), and covalent organic frameworks represent one of the extensively investigated classes of compounds in view of their utility for a variety of applications. Besides the principal utility in the areas of gas storage,[1] catalysis,[2] and drug delivery,[3] these solids have been employed for chemical separation[4] and molecular sensing[5] as well. More recently, the encapsulation of diverse guest molecules by these porous materials, ranging from biomolecules or drug molecules to simple inorganic ions, has been reported, albeit at times with limited success.[6] The pore aperture properties play a crucial role in exhibiting selectivity toward a specific class of molecules, which may navigate through or stay within the cavities/voids of these extended solids.[7] The pore size has been successfully modulated by the choice of organic linkers used in the case of MOFs, although beyond a certain length of the linker, interpenetration is a common phenomenon, leading to diminished porosity.[8] Besides the size, the shape and dimensionality of the pores within these solids also change their properties and utilities.[9]

We have been investigating metallophosphate chemistry in recent times in great detail from structural, mechanistic, and possible applications points of view.[10] In this regard, we have recently reported on the usage of discrete D4R metallophosphate cages for the sensing and scavenging of fluoride ions.[11] A few examples of fluoride-ion-encapsulated D4R cages that are not phosphate-based have also been realized in the past.[12] It has further been shown that D4R zinc phosphates can be linked by N,N′-ditopic linkers of varying length into three-dimensional (3D) assemblies, resulting in framework solids with significant porosity and gas adsorption properties.[13] While the D4R cubanes themselves are capable of encapsulating fluoride ions, the framework solids synthesized by using 4,4′-bipyridine (BIPY) as the ditopic linker are incapable of hosting smaller ions and molecules.[13] In an attempt to overcome this deficiency and synthesize D4R zinc phosphate based MOFs, which can be employed as host lattices for small molecular species, the N,O-ditopic ligand 4,4′-bipyridine-*N*-oxide (BIPYMO) has been used

A

as the linker in the present investigation. Details of this study for sensing purposes, describing the synthesis of two-dimensional (2D) or 3D porous coordination polymers and their ability to selectively host fluoride ions or benzil molecules inside the intra- or intercubane cavities, respectively, are described in this contribution.

2. RESULTS AND DISCUSSION

2.1. BIPYMO as the Ditopic Spacer. The use of BIPY as a bridging ligand to form coordination polymers is well established in the literature through more than 6500 crystal structures recorded in the CSD based on BIPY (Figure 1).[14] The oxidized
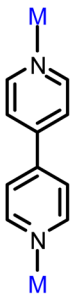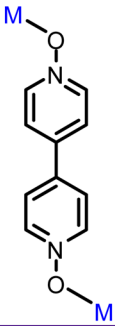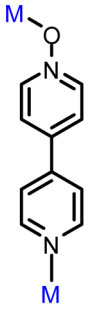

Figure 1. BIPY, BIPYDO, and BIPYMO binding modes displaying the deviation of oxygen-bound metal ions from the N−N axis of the ligand and the relative occurrence of these compounds as ligands in the CSD.

and more flexible 4,4′-bipyridine-*N,N*′-dioxide (BIPYDO), capable of forming angular coordination bonds because ligation is through oxygen, has emerged as a versatile supramolecular linker in recent times (∼300 hits in the CSD).[15] The third form, BIPYMO (**1**), which combines ligation by a nitrogen sp[2] center and an oxygen center, that is capable of displaying angles from 110 to 160° on the two ends of the same ligand, has been investigated only recently.[16] Its potential as a supramolecular synthon has not yet been explored in detail (Figure 1).[16]

The use of this ligand system in zinc phosphate chemistry would especially be interesting based on the hypothesis that the nitrogen and oxygen terminals would behave quite differently not only in terms of the electronic effects but also in terms of the bond angles possible at the ligating atoms. This can, in turn, lead to the isolation of newer types of framework structures that are different from those isolated using BIPY as the linker.[13]

The BIPYMO ligand was prepared by a protocol that is slightly different from an earlier published synthetic procedure where *m*-chloroperoxybenzoic acid was used as the oxidant.[16a] In the present study, the oxidation of BIPY has been carried out by 35% H_2O_2 in glacial acetic acid, followed by extraction with water and recrystallization in an ethyl acetate/methanol (9:1, v/v) solution. The crystalline off-white solid **1** (30% yield) has been characterized by analytical and spectroscopic methods. Four doublets in ^{1}H NMR with equal peak integrals, at δ 7.60, 7.80, 8.30, and 8.50 ppm, correspond to four sets of aromatic protons of **1** (Figure S1). The peak at *m/z* 173.07 in the mass spectrum in the Supporting Information corresponds to the $[M + H]^+$ molecular ion (Figure S2).

2.2. Synthesis and Spectral Characterization of [Zn₄(X-dipp)₄(BIPYMO)₂]·2MeOH [X = H (2), Cl (3), Br (4), I (5)]. A one-pot reaction involving [Zn(OAc)₂·2H₂O], X-dippH₂, and BIPYMO in a 1:1:1 ratio in methanol at room temperature for a few hours, followed by crystallization of the products by slow evaporation of the solvent, yields products **2−5** as single crystals (Scheme 1, path A). Frameworks **2−5** can also be prepared by treating the preformed D4R zinc phosphates [Zn(X-dipp)(DMSO)]₄[13,17] with BIPYMO in methanol (Scheme 1, path B). The new products have been characterized by both analytical and spectroscopic methods. The composition of the new compounds could be easily derived from their elemental analysis values. The phase purity of all of the new compounds has been investigated by powder X-ray diffraction (PXRD) of the vacuum-dried bulk samples. It appears that, because of the rapid loss of lattice solvent molecules from compounds **3** and **4**, there is a change in the crystal structure, and hence some discrepancy has been observed between the simulated and experimental PXRD patterns. Hence, PXRD measurements of **3**, **4**, and **7** were repeated using freshly crystallized samples that are only air-dried. These measurements yield diffraction patterns that match the simulated patterns. In the case of **6**, however, the crystal removed from the mother liquor leads to immediate amorphization, yielding very poor PXRD results (Figures S3−S6).

The Fourier transform infrared (FT-IR) spectra of **2−5** recorded as KBr-diluted thin disks show strong absorption bands at 1174, 1016, and 919 cm⁻¹ for **2**, 1178, 1017, and 921 cm⁻¹ for **3**, 1178, 1017, and 918 cm⁻¹ for **4**, and 1182, 1018, and 913 cm⁻¹ for **5**, corresponding to the O−P−O stretching and M−O−P asymmetric and symmetric vibrations, respectively. The absence of any absorption around 2350 cm⁻¹ implies that there are no free P−OH groups on the aryl phosphate ligands in **2−5** (Figure S7). Frameworks **2−5** are insoluble in most organic solvents except in dimethyl sulfoxide (DMSO). Hence, NMR characterization of the products was carried out in a DMSO solution. It should, however, be noted that zinc phosphate frameworks upon dissolution in DMSO decompose back to cubanes that contain DMSO ligands on the zinc centers (**A**) and free ditopic spacer ligands[10a] (Scheme 1, path C). The ^{1}H NMR spectra of **2−5** exhibit well-separated resonances for all of the protons of phosphate and BIPYMO ligands with a peak integral ratio of 2:1, affirming the role of BIPYMO as the bridging ligand in **2−5** (Figure S8). The presence of four doublets in the region 7.8−8.7 ppm corresponds to the aryl protons of BIPYMO, and the singlet observed around 7.0 ppm corresponds to aryl protons of the phosphate ligands. In the case of **2**, multiplets are observed in the same region. Further, a multiplet and a doublet observed at around 3.5 and 1.0 ppm correspond to the methine and methyl protons of the phosphate ligands, respectively. A single resonance is observed at −5.20, −5.38, −5.47, and −5.52 ppm in the ^{31}P NMR spectra of **2−5** in DMSO, respectively (Figure S9), corresponding to the formation of species **A** in a DMSO-*d₆* solution (Scheme 1).

2.3. Molecular Structures of 3 and 4. Single crystals of **2−5** have been isolated directly from the reaction mixtures by the slow evaporation of solvent at room temperature. While the crystals obtained for **3** and **4** have been found to be suitable for X-ray diffraction, crystals of **2** and **5** did not diffract well. Hence, the structures of **3** and **4** have been determined as representative examples for this series of zinc phosphates. Compounds **3** and **4** are isomorphous and crystallize in the tetragonal space group *P*4₁2₁2. A perspective view of the molecular structure of the

Scheme 1. Synthesis of BIPYMO-Based Zinc Phosphate 2D and 3D Frameworks 2−7
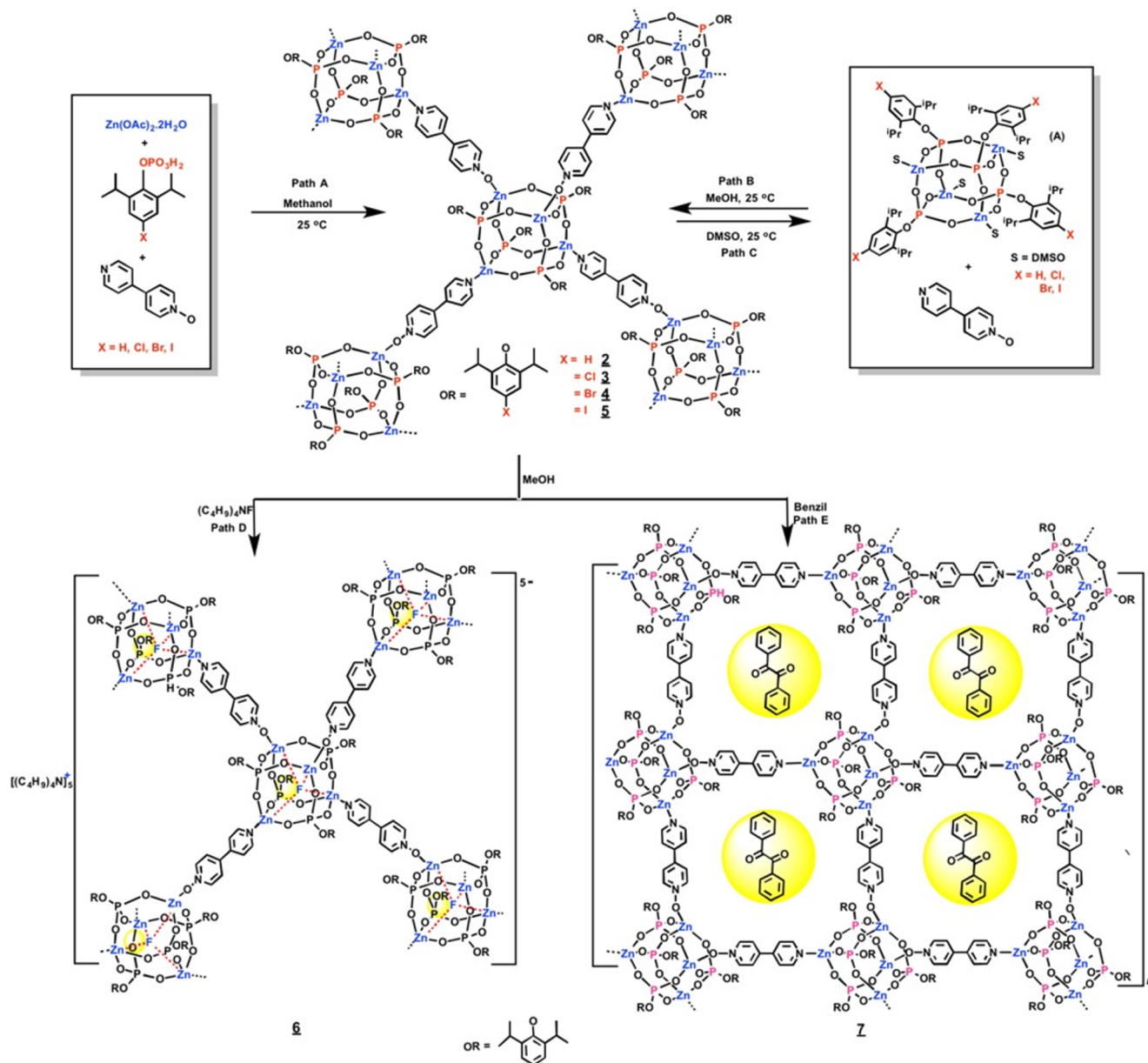
repeating unit of these framework compounds is shown in Figure 2.

The D4R zinc phosphate secondary binding units (SBUs) in **3** and **4** consist of zinc and phosphorus vertices that are bridged by a μ_2-oxygen atom. Both zinc and phosphorus centers adopt a nearly tetrahedral geometry with average bond angles of 109.54° and 109.46°, respectively. The average P−O(Zn) bond lengths in **3** and **4** are 1.491 and 1.512 Å, respectively, which are significantly shorter than a formal P−O single bond (1.60 Å) but considerably longer than P=O double-bond distances (1.45−1.46 Å).[19] Each of the six faces of the D4R SBUs is the eight-membered $Zn_2O_4P_2$ S4R rings that adopt a distorted pseudo-C_4 crown conformation, with the Zn−O−P angles in the ring ranging from 128.32(2) to 155.22(5)° in **3** and from 125.94(1) to 158.53(1)° in **4**. The dimensions of the D4R SBUs can best be understood from the lengths of the Zn···P edge (3.153 Å in **3** and 3.176 Å in **4**), P···P face diagonal (4.668 Å in **3** and 4.659 Å in **4**), Zn···Zn face diagonal (4.329 Å in **3** and 4.363 Å in **4**), and Zn···P

body diagonal (5.475 Å in **3** and 5.505 Å in **4**). The cage dimensions of **3** and **4** are comparable to those of other reported D4R zinc phosphates (Tables 1 and 2).[17]

In contrast to the 3D diamondoid frameworks obtained for BIPY-bridged zinc phosphate framework solids,[13] the solid-state structures of **3** and **4** reveal that these compounds are 2D coordination frameworks bridged by BIPYMO linkers (Figures 3 and S14 and S15). The ditopic BIPYMO linkers bridge the zinc centers of two neighboring D4R zinc phosphate cubanes by coordinating through the oxygen atom on the one end and the nitrogen atom on the other end. The Zn−O−N bond angle of around 120° implies that the oxygen atom of BIPYMO is in sp^2 hybridization, as has also been reported in the case of some N-oxide coordination compounds.[18] These bent Zn−O−N angles in **3** and **4** restrict them to form only a 2D framework, in contrast to the 3D frameworks formed when BIPY is used as the spacer with the same zinc phosphate building blocks.[13] The 8.379-Å-
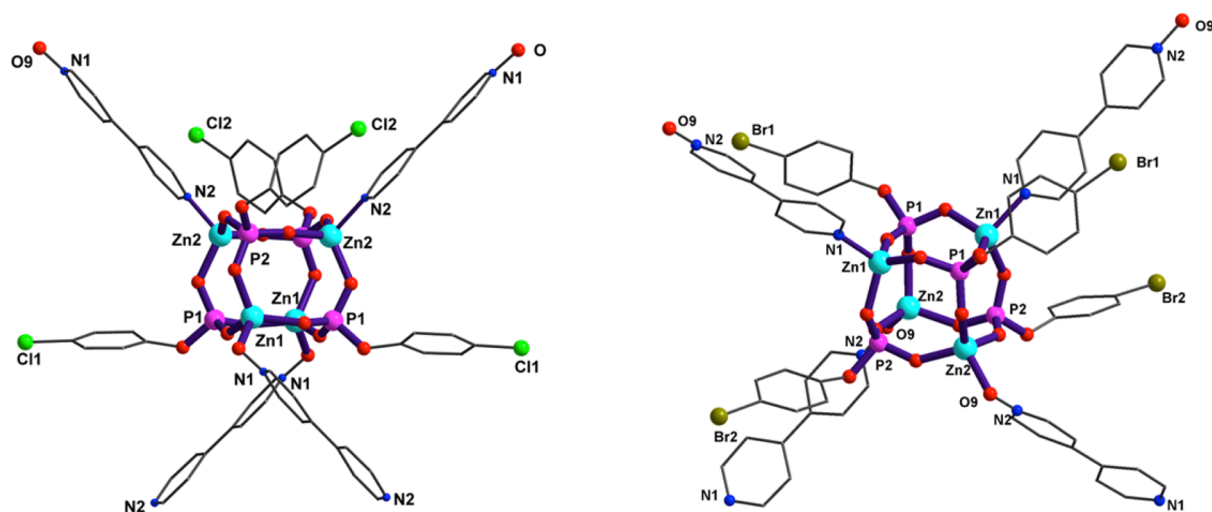
Figure 2. Molecular structure diagrams of **3** and **4** (isopropyl groups, hydrogen atoms, and lattice solvent molecules are omitted for the sake of clarity).

Table 1. Comparison of the Dimensions of Unfilled D4R Cubanes 3, 4, and 7 with Fluoride-Encapsulated 6

3 Average distances (Å)	**4** Average distances (Å)	**7** Average distances (Å)	**6** Average distances (Å)
Zn···P (edge) 3.153	Zn···P (edge) 3.176	Zn···P (edge), 3.213	Zn···P (edge), 3.063
Zn···Zn (face diagonal) 4.329	Zn···Zn (face diagonal) 4.363	Zn···Zn (face diagonal), 4.292	Zn···Zn (face diagonal), 3.791
P···P (face diagonal) 4.664	P···P (face diagonal) 4.659	P···P (face diagonal), 4.589	P···P (face diagonal), 4.832
Zn···P (body diagonal) 5.475	Zn···P (body diagonal) 5.505	Zn···P (body diagonal), 5.455	Zn···P (body diagonal), 5.255
			Zn···F, 2.305
			P···F, 2.935

Table 2. Comparison of the Structural Parameters of 3, 4, 6, and 7 with Those Found for Earlier Reported D4R Zinc Phosphates

formula	Zn−O [Å]	Zn−N [Å]	Zn···P [Å]	Zn−O−P [deg]	face diagonal		body diameter [Å]	Zn−O−N [deg]
					Zn···Zn [Å]	P···P [Å]		
[Zn(dippH$_2$)(collidine)]$_4$[10]	1.916		3.196		4.419	4.632	5.529	
[Zn(dippH$_2$)(2-apy)]$_4$·2MeOH[10]	1.923		3.179		4.347	4.598	5.477	
[Zn(Cl-dippH$_2$)(collidine)]$_4$[15]	1.921		3.197		4.471	4.527	5.536	
[Zn(Cl-dippH$_2$)(2apy)]$_4$·2MeOH[15]	1.933		3.175		4.447	4.541	5.544	
[Zn$_4$(Cl-dipp)$_4$(BIPYMO)$_2$]$_n$·2H$_2$O (**3**)	1.916	2.043	3.175	134.22	4.328	4.618	5.485	119.76
[Zn$_4$(Br-dipp)$_4$(BIPYMO)$_2$]$_n$·2H$_2$O (**4**)	1.925	2.042	3.195	135.28	4.371	4.629	5.495	123.29
[{(C$_4$H$_9$)$_4$N}$^+${F@Zn$_4$(dipp)$_4$(BIPYMO)$_2$}]$_n$ (**6**)	1.955	2.131	3.063	126.51	3.795	4.767	5.255	119.36
[benzil@{Zn$_4$(dipp)$_4$(BIPYMO)$_2$}]$_n$ (**7**)	1.895	2.055	3.213	125.25	4.292	4.589	5.455	108.63, 120.62

long BIPYMO linker separates two bridged zinc centers of the neighboring D4R SBUs by 11.601 Å.

The gas adsorption measurements have been carried out at 77 K. As-synthesized materials were dried under vacuum at 70−80 °C for 24 h to remove adsorbed solvent molecules, after appropriate solvent exchange. Brunauer−Emmett−Teller sur-

face area values for these compounds were found to be insignificant, ca. 30, 3.4, 2.4, and 1.7 m^2/g for **2**−**5**, respectively (Figures S10−S13), suggesting that the intercubane voids in these 2D frameworks are inaccessible, probably because of the bulky aryloxide ligands on the phosphorus. Hence, the possibility
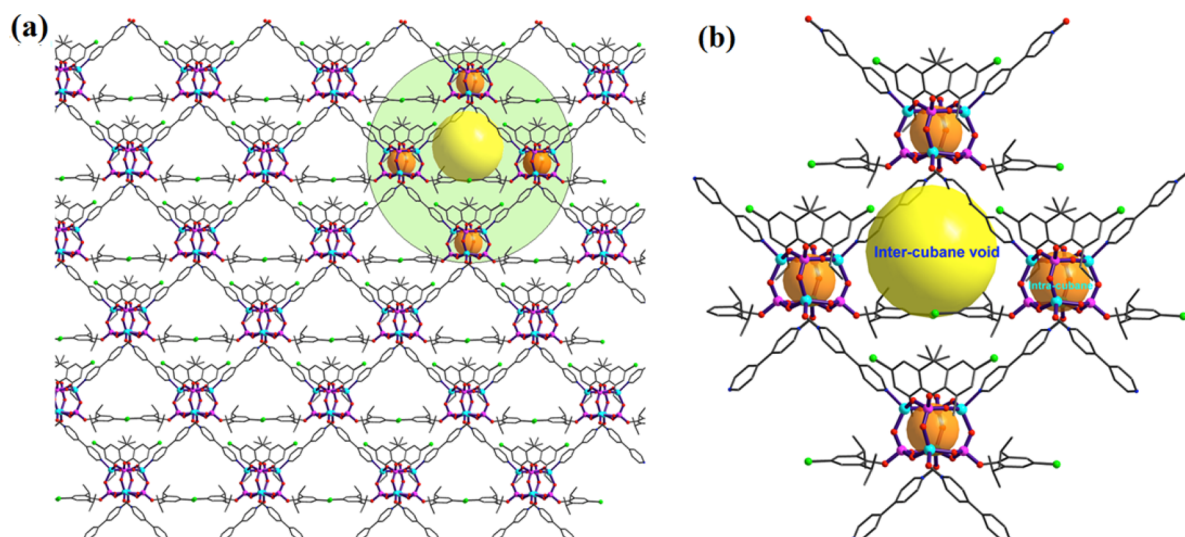
Figure 3. (a) Section of **3** showing linking of D4R SBUs by BIPYMO into 2D networks (down the *c* axis). (b) Possible intracubane (orange spheres) and intercubane (yellow spheres) voids in **3** (down the *c* axis).
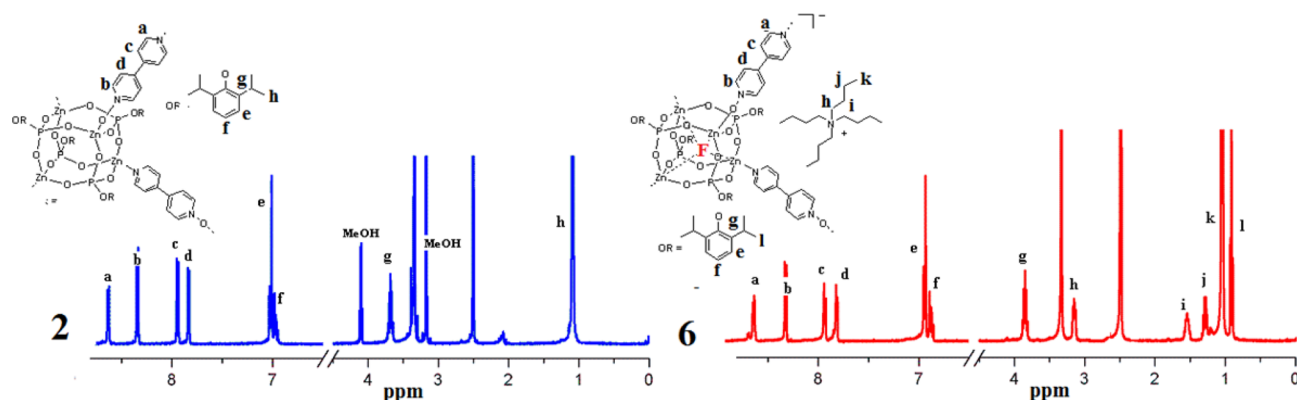

Figure 4. ^{1}H NMR (DMSO-d_6, 500 MHz) spectra of (left) fluoride-free framework **2** and (right) fluoride-ion-encapsulated framework **6**.

of intracubane voids (orange spheres in Figure 3b), rather than intercubane voids, for encapsulation has been investigated.

2.4. Fluoride-Encapsulated Phosphate Framework, {[(nC$_4$H$_9$)$_4$N][F@(Zn$_4$(dipp)$_4$(BIPYMO)$_2$)]}$_n$ (6). Discrete D4R cages are analogues of single-pore zeolitic entities, and hence several types of D4R cages have been investigated for the encapsulation of fluoride ions during the formation stages of these clusters,[12] including our recent demonstration that D4R zinc phosphates can selectively sense and encapsulate fluoride ions from various sources.[11] Because framework compounds **2**–**5** are 2D networks of D4R zinc phosphates, it will be interesting to probe the utility of these compounds for fluoride-ion sensing/encapsulation. Being soluble only in DMSO, the postsynthetic utility of **2**–**5** for the encapsulation of fluoride ions in solution is ruled out because it has been established recently that in DMSO such framework compounds do not remain intact but decompose to DMSO-decorated cubanes [Zn(dipp)(DMSO)]$_4$ and free ditopic spacer ligands.[10a] Therefore, the in situ generated frameworks **2**–**5** have been examined for fluoride-ion recognition/encapsulation studies. A one-pot reaction of zinc acetate, X-dippH$_2$ (X = H), and BIPYMO with tetrabutylammonium fluoride [1 M solution in tetrahydrofuran (THF)] in methanol at ambient conditions yielded fluoride-encapsulated framework **6** as a crystalline product after allowing the reaction mixture to stand undisturbed for 1 week at room temperature

(Scheme 1, path D). The same reaction carried out using X-dippH$_2$ (X = Cl, Br, I) as the phosphate source did not result in fluoride-ion incorporation. The parahalogens of these phosphate ligands seem to sterically disfavor the fluoride encapsulation owing to the bulky tetrabutylammonium cations competing with the halogens for the same intercubane voids available in the resultant frameworks. Fluoride inclusion also does not take place when alkali- or alkaline-earth-metal fluorides are used, probably because of the poor solubility of these halides in organic solvents.

The FT-IR spectrum of **6** does not exhibit any absorption at around 2350 cm^{-1}, indicating the absence of any free P–OH groups of the phosphate ligands. The strong absorptions observed at around 1157, 1045, and 910 cm^{-1} arise due to the O–P–O stretching and M–O–P asymmetric and symmetric stretching vibrations, respectively (Figure S16). The ^{1}H NMR spectrum shows well-separated signals for all of the protons of BIPYMO, phosphate ligand, and counterion [(C$_4$H$_9$)$_4$N]$^+$ in a 1:2:4 ratio, as suggested by the peak integral ratio of the NMR signals (Figure 4). The ^{31}P NMR spectrum in DMSO-d_6 (the only solvent in which **6** dissolves through DMSO complexation, releasing BIPYMO in solution) exhibits a single resonance at 2.97 ppm, which represents a downfield shift of about 8 ppm, compared to the chemical shift of the empty framework **2** (Figure S17). The ^{19}F NMR spectrum also exhibits a single resonance at −113 ppm (Figure S18). The ^{31}P and ^{19}F chemical shift values

are characterictic for fluoride encapsulated within the D4R zinc phosphate cage.[11]

2.5. Molecular Structure of 6. Single crystals of **6** were obtained by slow evaporation of the solvent. Single-crystal X-ray structure determination reveals that **6** crystallizes in the tetragonal space group $I\bar{4}2d$. The crystal structure of **6** (Figures 5 and 6) displays two major differences compared to the parent
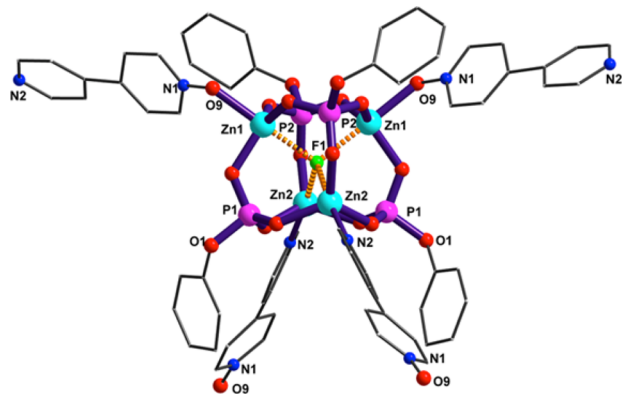

Figure 5. Molecular structure of compound **6** (hydrogen atoms, the isopropyl of the aryl ring, and counterion $[(C_4H_9)_4N]^+$ are omitted for clarity).

compounds **2**−**5**: (i) the intra-D4R cubane voids in **6** are filled with fluoride anions, and the tetra-n-butylammonium cations occupy the intercubane voids; (ii) the framework structure of **6** is 3D, in contrast to the 2D structures of **2**−**5**. Thus, compound **6** is a 3D network of fluoride-ion-encapsulated D4R zinc phosphate cubanes $[F@D4R]^-$, which are bridged by BIPYMO linkers.

Each of the anionic $[F@D4R]^-$ cages consists of four zinc atoms, four phosphate ligands, and an encapsulated fluoride ion. The fluoride ion is placed inside the D4R cage closer to the Zn1 centers [Zn1−F 2.258(1) Å] than to the Zn2 centers [Zn2−F 2.373(1) Å]. The observed Zn−F distances (Zn−F covalent bond ~1.775 Å) imply weak but significant interaction between the zinc and fluoride centers, leading to a change in the geometry about zinc from tetrahedral in the empty D4R zinc phosphates to trigonal-bipyramidal. The distance between the fluoride ion and phosphorus centers is, however, longer [P1−F1 2.931(1) Å and P2−F1 2.946(1) Å] and is almost twice that of the P−F distance in PF_5 (~1.56 Å as in PF_3),[20] suggesting no significant interaction between the phosphorus and encapsulated fluoride ions. This is also reflected in only a small shift in the ^{31}P chemical shift value of the encapsulated cubanes.[10a]

The phosphorus centers are in tetrahedral geometry with an average O−P−O bond angle of 109.24°. The presence of a fluoride ion distorts the D4R cages, drawing the zinc vertices inside and shortening the average Zn···Zn face diagonal to 3.795 Å, while the average P···P face diagonal is slightly elongated (4.767 Å). The distortion is further evident by comparable face diagonals (Zn···Zn ~ 4.450 Å and P···P ~ 4.610 Å). Selected bond parameters of **6** are compared with those of **3** and **4** and other earlier reported D4R zinc phosphates in Tables 1 and 2.

The bulky organic counterions $[(nC_4H_9)_4N]^+$, which occupy the intercubane voids, are highly disordered and could not be modeled. Because they are only physically held within the framework voids of **6** and do not involve any chemical interactions, they have been squeezed during refinement. It is worth noting that, in **6**, the BIPYMO groups bridge the anionic $[F@D4R]^-$ cages to form a 3D network (Figure 6), unlike the

empty frameworks **3** and **4**, which are 2D sheets. The increase in the dimensionality of **6** can be attributed to possible steric hindrance/congestion, resulting from bulky $[(C_4H_9)_4N]^+$ ions and a slight change of the angles around the zinc centers of the cubane (Figure S19).

2.6. Synthesis and Characterization of [benzil@(Zn₄(dipp)₄(BIPYMO)₂)]ₙ (7). The larger intercubane voids in the 2D framework compounds **2**−**5** have been probed for recognition of small organic molecules. The host framework of **2**, generated in situ by the reaction of $[Zn(OAc)_2 \cdot 2H_2O]$, X-dippH₂ (X = H), and BIPYMO in methanol, when treated with a mixture of benzene, toluene, aniline, benzoic acid, naphthalene, anthracene, benzidine, benzophenone, benzil, α-pyridoin, 1,2-diphenylethane-1,2-diamine, etc., yielded the benzil-encapsulated framework **7** as the only product.

Moreover, when treated independently with these organic molecules, the host framework was found to be selective for benzil, and when other small molecules were used, only empty frameworks were obtained. Compound **7**, the benzil-included **2**, has been characterized by analytical as well as spectroscopic methods.

The FT-IR spectral data for **7** is similar to **2**−**6**, with a prominent additional C=O stretching absorption at 1661 cm^{-1} (Figure S20). The ^{31}P NMR spectrum shows a single resonance at −5.23 ppm (Figure S21). The ^1H NMR spectrum shows well-separated peaks for dipp, BIPYMO, and benzil moieties and suggests the presence of these molecules in a 4:2:1 ratio (Figure S22).

2.7. Molecular Structure of 7. A single-crystal X-ray diffraction study reveals that **7** crystallizes in the triclinic space group $P\bar{1}$. A perspective view of the molecular structure and the packing diagram of **7** are shown in Figures 7 and 8, respectively (also see Figure S23). Unlike fluoride-encapsulated **6**, compound **7** retains the 2D skeleton of the host framework. The host framework of **7** is similar to empty frameworks of **3** and **4**, consisting of D4R zinc phosphates bridged by BIPYMO linkers. Various bond parameters of **7** are compared with the empty and fluoride-encapsulated compounds in Tables 1 and 2.

Like free benzil, the benzil molecules occluded within **7** also exist in the trans configuration (Figures 9 and S24) because the cis form is energetically not favored because of the steric hindrance by aryl rings.[19] The torsion angles between two aryl and carbonyl groups are C78−C77−C76−C69 172.36(7)°, C82−C77−C76−C69 1.09(1)°, C77−C76−C69−C70 −86.84(2)°, and O19−C76−C69−O20 −86.88(1)°. The bond parameters observed for the encapsulated benzil molecule do not deviate significantly from those of the free molecule.[21]

Structural analysis of **7** reveals two possible reasons for the observed selective encapsulation of benzil molecules by in situ formed host molecule **2**, over other closely related analogues: (a) the shape selectivity of the host and (b) both of the aryl rings of benzil are involved in significant strong π−π interactions with the aryl rings of the framework BIPYMO linkers (Figure 9).

2.8. Thermal Analysis. As has been described in section 2.2, the vacuum-dried samples lose lattice solvent molecules readily and, hence, thermogravimetric analyses of **2**−**7** have been carried under a N₂ atmosphere at a heating rate of 10 °C/min for both air-dried and vacuum-dried samples. The weight loss of ~60% in the temperature range of 100−550 °C corresponds to the loss of organic moieties, i.e., BIPYMO and 2,6-diisopropylphenyl groups, to produce $[ZnO_3P(OH)]$ in **2**−**5**, while in the guest-encapsulated framework compounds **6** and **7**, the first weight loss (beginning at 200 and 250 °C, respectively) can be attributed to
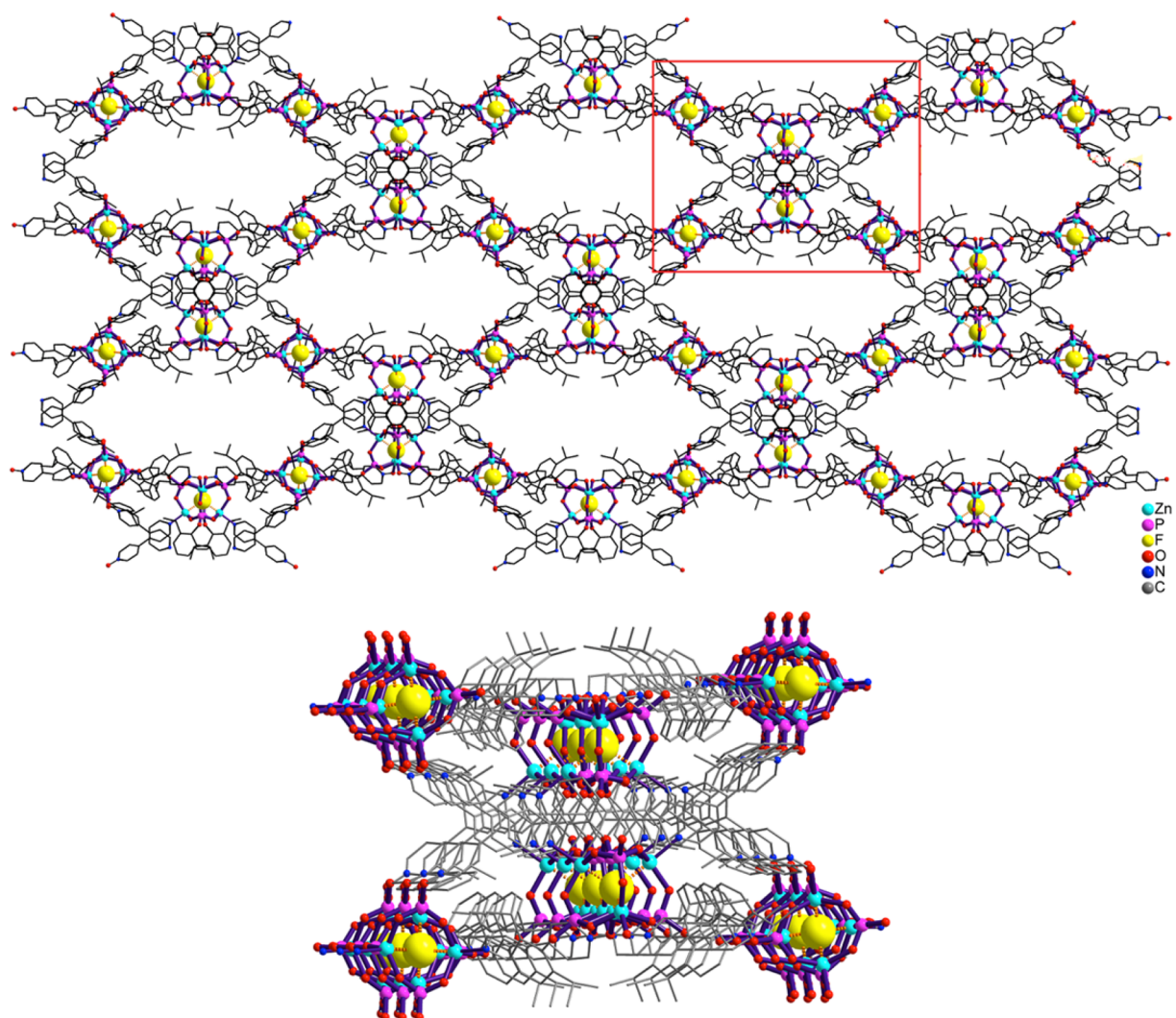
Figure 6. Framework structure of **6**. The yellow spheres represent fluoride ions inside D4R cages (down the *b* axis).
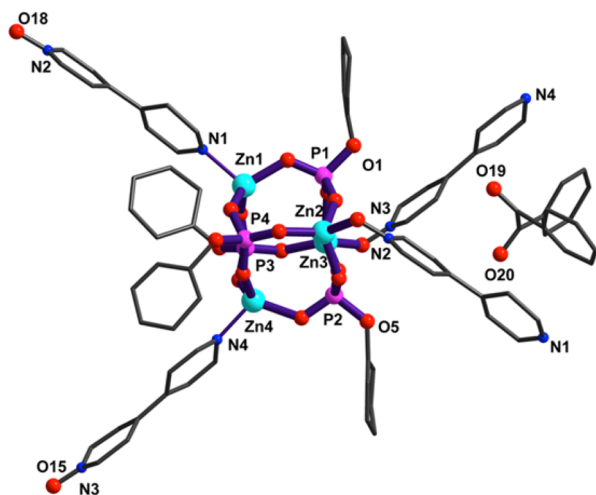

Figure 7. Molecular structure diagram of **7** (along the *b* axis; hydrogen atoms and isopropyl groups of the aryl ring of the phosphate ligand are omitted for clarity).

the loss of loosely bound tetrabutylammonium and benzil molecules. Upon heating to 1000 °C, condensation of [ZnO$_3$P-(OH)] with the loss of water molecules takes place, leading to the

formation of pyrophosphate Zn$_2$P$_2$O$_7$. The air-dried samples also behave in a similar manner but for a small weight loss observed at temperatures of less than 200 °C, corresponding to the amount of lattice solvent present in the system (Figures S25 and S26).

3. CONCLUSIONS

Zinc phosphate based extended coordination polymers have been designed and synthesized. Their utility as versatile molecular hosts has also been demonstrated. 2D networks **2−5** have been made accessible via both in situ and postsynthetic methods employing an uncommon ditopic linker, BIPYMO. Interestingly, compared to 3D frameworks of D4R zinc phosphates reported with BIPY,[13] the partially oxidized form BIPYMO integrates the D4R zinc phosphates into 2D sheets. The structural analyses of **3** and **4** reveal the presence of two types of voids (intra- and intercubane), which have been shown to be selective for fluoride ions and benzil molecules, respectively. The framework **6** represents a very rare example of a structurally characterized coordination polymer/MOF with encapsulated fluoride ions. The intercubane voids are highly selective for benzil molecules, owing to shape selectivity as well as π−π interactions with the host framework.
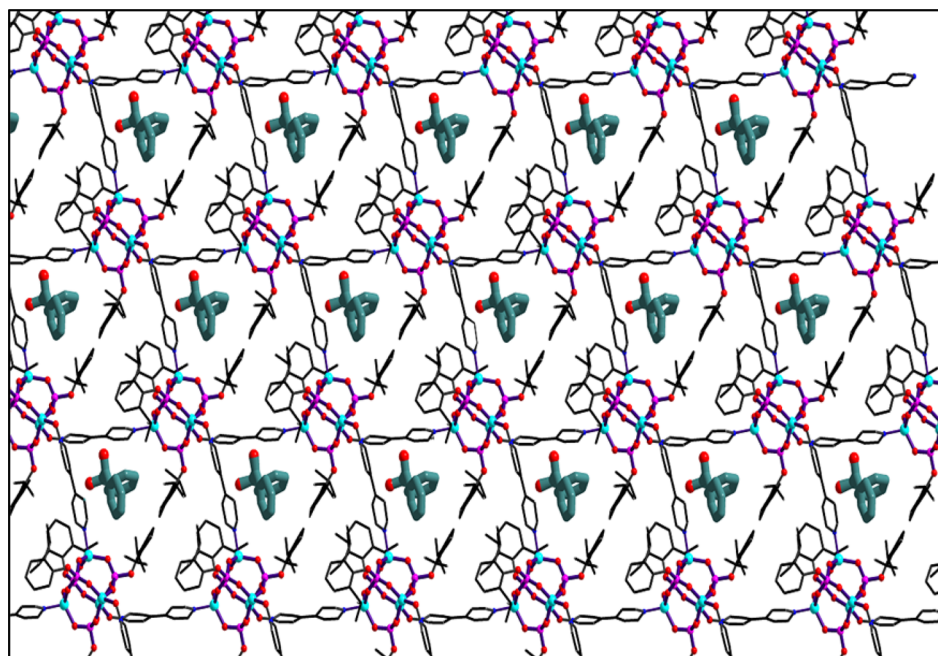
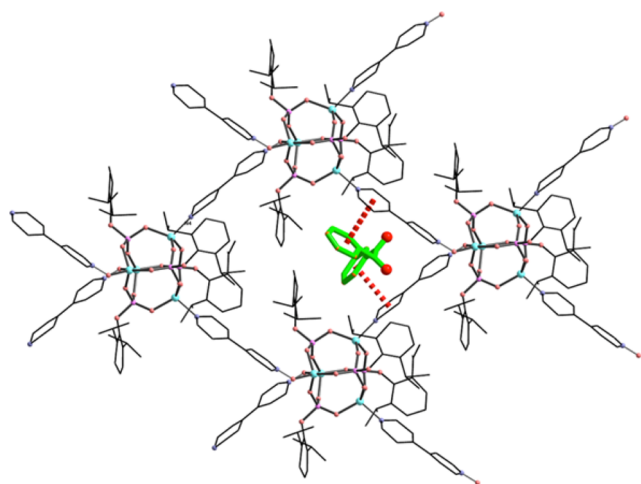**Figure 8.** 2D framework illustration of **7** (viewed down the *c* axis).

Figure 9. Trans-configurational shape and $\pi-\pi$ interactions between the aryl rings of benzil and the BIPYMO linkers of the framework stabilizing the guest molecules in **7** (down the *c* axis).

4. EXPERIMENTAL SECTION

4.1. Methods and Materials. All reactions were carried out at ambient reaction conditions. Melting points were measured in glass capillaries and are reported uncorrected. FT-IR spectra were obtained on a PerkinElmer Spectrum One spectrometer as KBr-diluted disks. Microanalyses were performed on a Thermo Finnigan (FLASH EA 1112) microanalyzer. The ^{1}H (Me$_4$Si internal standard), ^{31}P (85% H$_3$PO$_4$ external standard), and ^{19}F NMR spectra were recorded on a Bruker Advance DPX-500 spectrometer. Thermogravimetric analyses were carried out on a PerkinElmer Pyris thermal analysis system, under a stream of nitrogen gas at a heating rate of 10 °C/min. Solvents were purified according to standard procedures and distilled prior to use.[20] Solid-state absorption studies were carried out on a Varian Cary Eclipse spectrofluorimeter. Commercially available starting materials such as 4,4′-bipyridine (BIPY; Sigma-Aldrich), tetra-*n*-butylammonium fluoride (TBAF; 1 M THF, Sigma-Aldrich), benzil (Merck), toluene (Merck), aniline (Merck), benzoic acid (Merck), naphthalene (Merck), anthracene (Sigma-Aldrich), benzidine (Sigma-Aldrich), benzophenone (Sigma-Aldrich), benzil (Sigma-Aldrich), α-pyridoin,1,2-diphenyl-

ethane-1,2-diamine, and [Zn(OAc)$_2$·2H$_2$O] (s.d. Fine-Chem) were used as procured. 2,6-Diisopropylphenyl phosphate (dippH$_2$), 4-chloro-2,6-diisopropylphenyl phosphate (Cl-dippH$_2$), 4-bromo-2,6-diisopropylphenyl phosphate (Br-dippH$_2$), and 4-iodo-2,6-diisopropylphenyl phosphate (I-dippH$_2$) were synthesized as described previously.[21]

4.2. Synthesis of 1. To a solution of BIPY (16.5 mmol, 2.60 g) in 15 mL of glacial acetic acid was added 1.25 cm^3 of 35% aqueous H$_2$O$_2$, and the mixture was heated at 70−75 °C. After 3 h, another 0.17 cm^3 of 35% H$_2$O$_2$ was added, and the reaction was continued for additional 9 h at the same temperature. The solvent was removed on a rotary evaporator, and the residue was made alkaline with a saturated aqueous solution of sodium carbonate and washed with chloroform. The extracted aqueous phase yielded an off-white crystalline compound by the slow evaporation of solvent at room temperature after 3 days, which upon recrystallization in an ethyl acetate/methanol (9:1 v/v) solution yielded **1** as a crystalline solid. Yield: 0.86 g (30%). Mp: 135 °C. ^{1}H NMR (D$_2$O, 400 MHz): δ 7.60 (d, $^3J_{HH}$ = 4.1 Hz, 2H, *m*-NO), 7.80 (d, $^3J_{HH}$ = 7.0 Hz, 2H, *m*-N), 8.30 (d, $^3J_{HH}$ = 7.0 Hz, 2H, *o*-NO), 8.50 (d, $^3J_{HH}$ = 4.2 Hz, 2H, *o*-N). HRMS (ESI). Calcd for C$_{10}$H$_8$N$_2$O: *m/z* 172.06. Found: *m/z* 173.07 ([M + H]$^+$).

4.3. Synthesis of 2−5. To a stirred solution of [Zn(OAc)$_2$·2H$_2$O] (0.25 mmol, 0.055 g) and X-dippH$_2$(0.25 mmol; X = H, 0.062 g; X = Cl, 0.073 g; X = Br, 0.084 g; X = I, 0.096 g) in methanol was added a solution of BIPYMO (0.13 mmol, 0.022 g) in methanol at 25 °C. The filtered solution yielded **2−5** as single crystals after 1 week. The framework compounds were also synthesized by the reaction of [Zn(X-dipp)-(DMSO)]$_4$ (0.25 mmol) in methanol with BIYPYMO (0.13 mmol) at room temperature.

2. Yield: 0.63 g (60%). Mp: >250 °C. Elem anal. Calcd for C$_{68}$H$_{88}$N$_4$O$_{20}$P$_4$Zn$_4$ (M_r = 1666.2): C, 49.01; H, 5.32; N, 3.36. Found: C, 49.52; H, 5.12; N, 3.41. IR (KBr, cm^{-1}): 2964 (s), 2867 (w), 1616 (s), 1481 (w), 1336 (s), 1174 (br), 1016 (s), 919 (w), 770 (w), 691 (w), 599 (w), 545 (w). ^{1}H NMR (DMSO-*d$_6$*, 500 MHz): δ 8.61 (d, 4H, bipy−H, $^3J_{HH}$ = 6.2 Hz), 8.35 (d, 4H, bipy−H,$^3J_{HH}$ = 7.4 Hz), 7.96 (d, 4H, bipy−H, $^3J_{HH}$ = 7.4 Hz), 7.84 (d, 4H, bipy−H, $^3J_{HH}$ = 6.2 Hz), 7.02 (d, 8H, Ar−H, $^3J_{HH}$ = 1.9 Hz), 6.96 (t, 4H, Ar−H, $^3J_{HH}$ = 6.2 Hz), 3.66 (septet, 8H, *i*Pr−CH, $^3J_{HH}$ = 6.8 Hz), 1.07 (d, 48H, CH$_3$, $^3J_{HH}$ = 6.8 Hz). ^{31}P NMR (DMSO-*d$_6$*, 202 MHz): δ −5.2. TGA [temp range, °C (weight loss, %)]: 30−331 (~3.0), 331−373 (~33.0), 373−511 (~26.0), 511−900 (~2.5), 900−1082 (~19.5).

3. Yield: 0.068 g (60%). Mp: >250 °C. Elem anal. Calcd for C$_{68}$H$_{84}$Cl$_4$N$_4$O$_{20}$P$_4$Zn$_4$ (M_r = 1804.7): C, 45.25; H, 4.69; N, 3.10.

Table 3. Crystal Data for Compounds 3, 4, 6, and 7

	3	4	6[a]	7
CCDC no.	1407144	1407145	1407146	1407147
empirical formula	$C_{36}H_{48}Cl_2N_2O_{11}P_2Zn_2$	$C_{36}H_{48}Br_2N_2O_{11}P_2Zn_2$	$C_{136}H_{168}FN_8O_{36}P_8Zn_8$	$C_{82}H_{89}N_4O_{20}P_4Zn_4$
fw	944.06	1037.34	3280.66	1836.02
temp [K]	293(2)	150(2)	150(2)	150(2)
cryst syst	tetragonal	tetragonal	tetragonal	triclinic
space group	$P4_12_12$	$P4_12_12$	$I\bar{4}2d$	$P\bar{1}$
a [Å]	15.7496(4)	15.7636(17)	27.581(5)	15.121(7)
b [Å]	15.7496(4)	15.7636(17)	27.581(5)	15.009(7)
c [Å]	35.8673(21)	36.843(4)	27.581(5)	21.587(9)
α [deg]				102.690(6)
β [deg]				102.475(2)
γ [deg]				109.882(6)
V [Å^3]	8896.8(6)	9155(2)	33067(1)	4263.0(3)
Z	8	8	4	2
D(calcd) [Mg/cm^3]	1.320	1.493	0.659	1.430
μ [mm^{-1}]	1.317	2.916	0.644	1.258
Θ range [deg]	3.36−25.00	2.81−25.00	2.62−25.00	2.59−25.00
no. of reflns collected	68638	68147	124089	31359
indep reflns [$I_0 > 2\sigma(I_0)$]	7815	8059	14558	14780
GOF	1.052	1.149	1.141	1.170
R1 [$I_0 > 2\sigma(I_0)$]	0.051	0.053	0.096	0.0770
wR2 (all data)	0.149	0.152	0.291	0.314

[a]Tetrabutylammonium cations [TBA]$^+$ in the channels are highly disordered and, hence, could not be modeled appropriately. Hence, they were squeezed during refinement.

Found: C, 45.45; H, 4.38; N, 3.21. IR (KBr, cm^{-1}): 3457 (br), 2965 (s), 2868 (w), 1616 (s), 1466 (b), 1336 (s), 1178 (br), 1017 (s), 921 (w), 827 (s), 697 (w), 599 (w), 547 (w). ^{1}H NMR (DMSO-d_6, 500 MHz): δ 8.62 (d, 4H, $^3J_{HH}$ = 6.2 Hz, bipy−H), 8.35 (d, 4H, $^3J_{HH}$ = 7.3 Hz, bipy−H), 7.94 (d, 4H, $^3J_{HH}$ = 7.3 Hz, bipy−H), 7.84 (d, 4H, $^3J_{HH}$ = 6.2 Hz, bipy−H), 7.02 (s, 8H, Ar−H), 4.10 (q, $^3J_{HH}$ = 5.2 Hz), 3.63 (septet, 8H, $^3J_{HH}$ = 6.8 Hz, ^{i}Pr−CH), 3.15 (d, $^3J_{HH}$ = 5.2 Hz), 1.09 (d, 48H, $^3J_{HH}$ = 6.8 Hz, CH$_3$). ^{31}P NMR (DMSO-d_6, 202 MHz): δ −5.4. TGA [temp range, °C (weight loss, %)]: 30−320 (~2.5), 320−470 (~56.5), 470−860 (~4.0), 860−1100 (~28.0).

4. Yield: 0.064 g (52%). Mp: >250 °C. Elem anal. Calcd for $C_{68}H_{84}Br_4N_4O_{20}P_4Zn_4$ (M_r = 1982.5): C, 41.20; H, 4.27; N, 2.83. Found: C, 41.67; H, 3.74; N, 2.88. IR (KBr, cm^{-1}): 3449 (br), 2964 (s), 2868 (w), 1617 (s), 1465 (b), 1336 (s), 1178 (br), 1017 (s), 918 (w), 803 (w), 691 (w), 599 (w), 545 (w). ^{1}H NMR (DMSO-d_6, 500 MHz): δ 8.61 (d, 4H, bipy−H, $^3J_{HH}$ = 6.2 Hz), 8.35 (d, 4H, bipy−H, $^3J_{HH}$ = 7.4 Hz), 7.96 (d, 4H, bipy−H, $^3J_{HH}$ = 7.4 Hz), 7.84 (d, 4H, bipy−H, $^3J_{HH}$ = 6.2 Hz), 7.15 (s, 8H, Ar−H), 4.10 (q, CH$_3$OH, $^3J_{HH}$ = 5.2 Hz), 3.63 (septet, 8H, ^{i}Pr−CH, $^3J_{HH}$ = 6.8 Hz), 3.15 (d, CH$_3$OH, $^3J_{HH}$ = 5.2 Hz), 1.09 (d, 48H, CH$_3$, $^3J_{HH}$ = 6.8 Hz). ^{31}P NMR (DMSO-d_6, 202 MHz): δ −5.5. TGA [temp range, °C (weight loss, %)]: 30−320 (~2.5), 320−510 (~60.0), 510−850 (~4.5), 850−1050 (~27.5).

5. Yield: 0.054 g (40%). Mp: >250 °C. Elem anal. Calcd for $C_{68}H_{84}I_4N_4O_{20}P_4Zn_4$ (M_r = 2170.5): C, 37.63; H, 3.90; N, 2.58. Found: C, 37.58; H, 3.73; N, 3.18. IR (KBr, cm^{-1}): 3406 (br), 2962 (s), 2866 (w), 1617 (s), 1441 (b), 1334 (s), 1182 (br), 1018 (s), 913 (w), 793 (w), 681 (w), 593 (w), 541 (w). ^{1}H NMR (DMSO-d_6, 500 MHz): δ 8.65 (d, 4H, bipy−H, $^3J_{HH}$ = 6.2 Hz), 8.32 (d, 4H, bipy−H, $^3J_{HH}$ = 7.4 Hz), 7.92 (d, 4H, bipy−H, $^3J_{HH}$ = 7.4 Hz), 7.80 (d, 4H, bipy−H, $^3J_{HH}$ = 6.2 Hz), 7.28 (s, 8H, Ar−H), 3.56 (septet, 8H, ^{i}Pr−CH, $^3J_{HH}$ = 6.8 Hz), 1.06 (d, 48H, CH$_3$, $^3J_{HH}$ = 6.8 Hz). ^{31}P NMR (DMSO-d_6, 202 MHz): δ −5.5. TGA [temp range, °C (weight loss, %)]: 30−320 (~2.5), 320−510 (~60.0), 510−875 (~4.5), 875−1090 (~27.52).

4.4. Synthesis of 6. To a solution of [Zn(OAc)$_2$·2H$_2$O] (0.40 mmol, 0.086 g) and dippH$_2$ (0.40 mmol, 0.102 g) in methanol (30 mL) was slowly added a solution of BIPYMO (0.20 mmol, 0.035 g) in methanol. A solution of TBAF (1 M THF; 0.40 mmol, 0.40 mL) in methanol was slowly added to the above reaction mixture, and **6** was obtained as a crystalline product after 1 week. Yield: 0.085 g (45%). Mp:

>250 °C. Elem anal. Calcd for $C_{84}H_{120}FN_5O_{18}P_4Zn_4$ (M_r = 1892.1): C, 53.31; H, 6.39; N, 3.70. Found: C, 53.34; H, 7.17; N, 4.56. IR (KBr, cm^{-1}): 3436 (br), 2962 (s), 2867 (m), 1613 (s), 1476 (s), 1256 (m), 1157 (s), 1045 (m), 996 (s), 910 (s), 771 (s), 565 (s). ^{1}H NMR (DMSO-d_6, 500 MHz): δ 8.65 (d, $^3J_{HH}$ = 5.19 Hz), 8.33 (d, $^3J_{HH}$ = 5.40 Hz), 7.94 (d, $^3J_{HH}$ = 5.42 Hz), 7.82 (d, $^3J_{HH}$ = 4.59 Hz), 6.94 (d, $^3J_{HH}$ = 7.0 Hz), 6.87 (t, $^3J_{HH}$ = 6.72 Hz), 5.74 (s), 3.84 (septet, $^3J_{HH}$ = 6.8 Hz), 3.15 (m, $^3J_{HH}$ = 3.08 Hz), 1.54 (m, $^3J_{HH}$ = 7.32 Hz), 1.30 (m, $^3J_{HH}$ = 7.37 Hz), 1.06 (d, $^3J_{HH}$ = 6.79 Hz), 0.91 (t, $^3J_{HH}$ = 7.39 Hz). ^{31}P NMR (DMSO-d_6, 202 MHz): δ 2.6. ^{19}F NMR (DMSO-d_6, 470 MHz): δ −113. TGA [temp range, °C (weight loss, %)]: 30−340 (~9.5), 340−511 (~44.0), 511−896 (~5.5).

4.5. Synthesis of 7. To a solution of [Zn(OAc)$_2$·2H$_2$O] (0.40 mmol, 0.086 g) and dippH$_2$ (0.40 mmol, 0.102 g) in methanol (30 mL) was slowly added a solution of BIPYMO (0.40 mmol, 0.069 g) in methanol. A solution of benzil (0.40 mmol) in methanol was added slowly to yield a clear solution, which yielded **7** as single crystals after 1 week. Compound **7** was obtained as the only product even when a solution of a mixture of organic molecules was added to the reaction mixture (viz., benzene, toluene, aniline, benzoic acid, naphthalene, anthracene, benzidine, benzophenone, benzil, α-pyridon, 1,2-diphenyl-ethane-1,2-diamine, etc.). Yield: 0.100 g (55%). Mp: >250 °C. Elem anal. Calcd for $C_{82}H_{94}N_4O_{20}P_4Zn_4$ (M_r = 1834.2): C, 53.49; H, 5.15; N, 3.04. Found: C, 52.45; H, 4.98; N, 3.04. IR (KBr, cm^{-1}): 3445 (br), 2964 (s), 2867 (m), 1661 (s), 1614 (s), 1450 (s), 1257 (m), 1170 (w), 1074 (s), 1012 (s), 915 (s), 770 (s), 529 (s). ^{1}H NMR (DMSO-d_6, 500 MHz): δ 8.64 (d, $^3J_{HH}$ = 5.76 Hz), 8.33 (d, $^3J_{HH}$ = 7.24 Hz), 7.93 (d, $^3J_{HH}$ = 7.17 Hz), 7.92 (d, $^3J_{HH}$ = 7.00 Hz), 7.81 (t, $^3J_{HH}$ = 6.00 Hz), 7.78 (d, $^3J_{HH}$ = 7.74 Hz), 7.61 (t, $^3J_{HH}$ = 8.04 Hz), 7.01 (d, $^3J_{HH}$ = 8.25 Hz), 7.96 (t, $^3J_{HH}$ = 6.32 Hz), 3.65 (septet, $^3J_{HH}$ = 6.77 Hz), 1.07 (d, $^3J_{HH}$ = 6.85 Hz). ^{31}P NMR (DMSO-d_6, 202 MHz): δ −5.2. TGA [temp range, °C (weight loss, %)]: 30−220 (~5.0), 220−700 (~64.0).

4.6. Single-Crystal X-ray Diffraction Studies. Single crystals of compounds **2**−**7** were directly obtained from the reaction mixture by slow evaporation of the solvent. The determination of the unit cell parameters and data collection were performed with Mo Kα radiation (λ = 0.7107 Å). Diffraction intensities were collected on a Rigaku Saturn 724+ CCD diffractometer, and data integration and indexing were carried out using *CrystalClear-SM Expert*. Various calculations were

carried out using *WinGX*.[22] The structures were solved by direct methods (*SIR-92*),[23] and the final refinement was carried out using full least-squares methods on F^2 using *SHELXL-97*.[24] Although multiple attempts were made, poor-quality crystals of **6** did not yield good diffraction data. The structure of **6** contains highly disordered [Bu$_4$N]$^+$ counterions that could not be precisely modeled and refined anisotropically. The lattice solvent molecules in **4** are disordered, and hence associated hydrogen atoms have not been identified or fixed. Details of the structure determination are reported in Table 3.

■ ASSOCIATED CONTENT

⑤ Supporting Information
The Supporting Information is available free of charge on the ACS Publications website at DOI: 10.1021/acs.inorgchem.5b02949.

> Synthesis, crystallographic details, additional figures, and spectral characterization (PDF)
> X-ray crystallographic data in CIF format (CIF)

■ AUTHOR INFORMATION

Corresponding Author
*Tel: +91 22 2576 7163. Fax: +91 22 2572 3480. E-mail: rmv@chem.iitb.ac.in.

Present Address
‡Department of Chemistry (Inorganic Branch), University of Kashmir, Hazratbal, Srinagar, J&K, 190006, India

Notes
The authors declare no competing financial interest.

■ ACKNOWLEDGMENTS

■ DEDICATION
†This paper is dedicated to the memory of Professor P. Natarajan.

■ REFERENCES

(1) (a) Galownia, J.; Martin, J.; Davis, M. E. *Microporous Mesoporous Mater.* **2006**, *92*, 61−63. (b) Breck, D. W. *Zeolite Molecular Sieves*; John Wiley & Sons Inc.: New York, 1974. (c) Yaghi, O. M.; O'Keeffe, M.; Ockwig, N. W.; Chae, H. K.; Eddaoudi, M.; Kim, J. *Nature* **2003**, *423*, 705−714. (d) Cote, A. P.; Benin, A. I.; Ockwig, N. W.; O'Keeffe, M.; Matzger, A. J.; Yaghi, O. M. *Science* **2005**, *310*, 1166−1170. (e) Alezi, D.; Belmabkhout, Y.; Suyetin, M.; Bhatt, P. M.; Weseliński, L. J.; Solovyeva, V.; Adil, K.; Spanopoulos, I.; Trikalitis, P. N.; Emwas, A.-H.; Eddaoudi, E. *J. Am. Chem. Soc.* **2015**, *137*, 13308−13318. (f) Huang, L.; Yang, X.; Cao, D. *J. Phys. Chem. C* **2015**, *119*, 3260−3267.

(2) (a) Park, J.; Li, J.-R.; Chen, Y.-P.; Yu, J.; Yakovenko, A. A.; Wang, Z. U.; Sun, L.-B.; Balbuena, P. B.; Zhou, H.-C. *Chem. Commun.* **2012**, *48*, 9995−9997. (b) Du, D.-Y.; Qin, J.-S.; Sun, Z.; Yan, L.-K.; O'Keeffe, M.; Su, Z.-M.; Li, S.-L.; Wang, X.-H.; Wang, X.-L.; Lan, Y.-Q. *Sci. Rep.* **2013**, *3*, 2616. (c) Gándara, F.; Gomez-Lor, B.; Gutiérrez-Puebla, E.; Iglesias, M.; Monge, M. A.; Proserpio, D. M.; Snejko, N. *Chem. Mater.* **2008**, *20*, 72−76. (d) Wang, J.-C.; Ding, F.-W.; Ma, J.-P.; Liu, Q.-K.; Cheng, J.-Y.; Dong, Y.-B. *Inorg. Chem.* **2015**, *54*, 10865−10872.

(3) (a) Horcajada, P.; Chalati, T.; Serre, C.; Gillet, B.; Sebrie, C.; Baati, T.; Eubank, J. F.; Heurtaux, D.; Clayette, P.; Kreuz, C.; Chang, J.-S.; Hwang, Y. K.; Marsaud, V.; Bories, P.-N.; Cynober, L.; Gil, S.; Férey, G.; Couvreur, P.; Gref, R. *Nat. Mater.* **2010**, *9*, 172−178. (b) Taylor-Pashow, K. M. L.; Rocca, J. D.; Xie, Z.; Tran, S.; Lin, W. B. *J. Am. Chem.*

Soc. **2009**, *131*, 14261−14263. (c) McKinlay, A. C.; Morris, R. E.; Horcajada, P.; Férey, G.; Gref, R.; Couvreur, P.; Serre, C. *Angew. Chem., Int. Ed.* **2010**, *49*, 6260−6266. (d) Taylor, K. M. L.; Rieter, W. J.; Lin, W. B. *J. Am. Chem. Soc.* **2008**, *130*, 14358−14389.

(4) (a) Singha, D. K.; Mahata, P. *Inorg. Chem.* **2015**, *54*, 6373−6379. (b) Li, H.-Y.; Wei, Y.-L.; Dong, X.-Y.; Zang, S.-Q.; Mak, T. C. W. *Chem. Mater.* **2015**, *27*, 1327−1331. (c) Lee, J. Y.; Farha, O. K.; Roberts, J.; Scheidt, K. A.; Nguyen, S. T.; Hupp, J. T. *Chem. Soc. Rev.* **2009**, *38*, 1450−1459. (d) Li, J. R.; Yu, J.; Lu, W.; Sun, L.-B.; Sculley, J.; Balbuena, P. B.; Zhou, H.-C. *Nat. Commun.* **2013**, *4*, 1538. (e) Sculley, J. P.; Zhou, H. C. *Angew. Chem., Int. Ed.* **2012**, *51*, 12660−12661.

(5) (a) Kreno, L. E.; Leong, K.; Farha, O. K.; Allendorf, M.; Van Duyne, R. P.; Hupp, J. T. *Chem. Rev.* **2012**, *112*, 1105−1125. (b) Perry, J. J.; Bauer, C. A.; Allendorf, M. D. Luminescent Metal−Organic Frameworks. In *Metal−Organic Frameworks: Applications from Catalysis to Gas Storage*; David, F., Ed.; Wiley-VCH Verlag GmbH & Co.: Weinheim, Germany, 2011; pp 267−308. (c) Lu, G.; Hupp, J. T. *J. Am. Chem. Soc.* **2010**, *132*, 7832−7833.

(6) (a) Jia, Y.; Wei, B.; Duan, R.; Zhang, Y.; Wang, B.; Hakeem, A.; Liu, N.; Ou, X.; Xu, S.; Chen, Z.; Lou, X.; Xia, F. *Sci. Rep.* **2014**, *4*, 5929. (b) Horcajada, P.; Serre, C.; Vallet-Regí, M.; Sebban, M.; Taulelle, F.; Ferey, G. *Angew. Chem., Int. Ed.* **2006**, *45*, 5974−5978. (c) Horcajada, P.; Chalati, T.; Serre, C.; Gillet, B.; Sebrie, C.; Baati, T.; Eubank, J. F.; Heurtaux, D.; Clayette, P.; Kreuz, C.; Chang, J.-S.; Hwang, Y. K.; Marsaud, V.; Bories, P.-N.; Cynober, L.; Gil, S.; Ferey, G.; Couvreur, P.; Gref, R. *Nat. Mater.* **2010**, *9*, 172−178. (d) Hermann, D.; Emerich, H.; Lepski, R.; Schaniel, D.; Ruschewitz, U. *Inorg. Chem.* **2013**, *52*, 2744−2749. (e) Serra-Crespo, P.; Ramos-Fernandez, E. V.; Gascon, J.; Kapteijn, F. *Chem. Mater.* **2011**, *23*, 2565−2572. (f) Bruns, C. J.; Fujita, D.; Hoshino, M.; Sato, S.; Stoddart, J. F.; Fujita, M. *J. Am. Chem. Soc.* **2014**, *136*, 12027−12034.

(7) (a) Jiang, H. L.; Feng, D. W.; Liu, T. F.; Li, J. R.; Zhou, H. C. *J. Am. Chem. Soc.* **2012**, *134*, 14690−14693. (b) Kuo, C.-H.; Tang, Y.; Chou, L. Y.; Sneed, B. T.; Brodsky, C. N.; Zhao, Z.; Tsung, C. K. *J. Am. Chem. Soc.* **2012**, *134*, 14345−14348. (c) Chapman, K. W.; Sava, D. F.; Halder, G. J.; Chupas, P. J.; Nenoff, T. M. *J. Am. Chem. Soc.* **2011**, *133*, 18583−18585. (d) Furutani, Y.; Kandori, H.; Kawano, M.; Nakabayashi, K.; Yoshizawa, M.; Fujita, M. *J. Am. Chem. Soc.* **2009**, *131*, 4764−4768.

(8) (a) Almeida Paz, F. A.; Klinowski, J.; Vilela, S. M. F.; Tome, J. P. C.; Cavaleiro, J. A. S.; Rocha, J. *Chem. Soc. Rev.* **2012**, *41*, 1088−1110. (b) Ma, S. Q.; Zhou, H. C. *J. Am. Chem. Soc.* **2006**, *128*, 11734−111735.

(9) Sun, C.-Y.; Wang, X.-L.; Qin, C.; Jin, J.-L.; Su, Z.-M.; Huang, P.; Shao, K.-Z. *Chem. - Eur. J.* **2013**, *19*, 3639−3645.

(10) (a) Dar, A. A.; Sen, S.; Gupta, S. K.; Patwari, G. N.; Murugavel, R. *Inorg. Chem.* **2015**, *54*, 9458−9469. (b) Walawalkar, M. G.; Roesky, H. W.; Murugavel, R. *Acc. Chem. Res.* **1999**, *32*, 117−126. (c) Murugavel, R.; Shanmugan, S. *Chem. Commun.* **2007**, 1257−1259. (d) Murugavel, R.; Shanmugan, S. *Dalton Trans.* **2008**, 5358−5367. (e) Murugavel, R.; Walawalkar, M. G.; Dan, M.; Roesky, H. W.; Rao, C. N. R. *Acc. Chem. Res.* **2004**, *37*, 763−774. (f) Murugavel, R.; Gogoi, N.; Clerac, R. *Inorg. Chem.* **2009**, *48*, 646−651. (g) Murugavel, R.; Kuppuswamy, S.; Boomishankar, R.; Steiner, A. *Angew. Chem., Int. Ed.* **2006**, *45*, 5536−5540. (h) Murugavel, R.; Kuppuswamy, S.; Gogoi, N.; Boomishankar, R.; Steiner, A. *Chem. - Eur. J.* **2010**, *16*, 994−1009. (i) Murugavel, R.; Kuppuswamy, S.; Gogoi, N.; Steiner, A. *Inorg. Chem.* **2010**, *49*, 2153−2162. (j) Murugavel, R.; Kuppuswamy, S. *Angew. Chem., Int. Ed.* **2006**, *45*, 7022−7026. (k) Murugavel, R.; Kuppuswamy, S.; Gogoi, N.; Boomishankar, R.; Steiner, A. *Chem. - Eur. J.* **2008**, *14*, 3869−3873. (l) Kalita, A. Ch.; Roch-Marchal, C.; Murugavel, R. *Dalton Trans* **2013**, *42*, 9755−9763. (m) Murugavel, R.; Kuppuswamy, S. *Inorg. Chem.* **2008**, *47*, 7686−7694. (n) Murugavel, R.; Kuppuswamy, S.; Randoll, S. *Inorg. Chem.* **2008**, *47*, 6028−6039. (o) Murugavel, R.; Kuppuswamy, S.; Maity, A. N.; Singh, M. P. *Inorg. Chem.* **2009**, *48*, 183−192. (p) Murugavel, R.; Sathiyendiran, M.; Walawalkar, M. G. *Inorg. Chem.* **2001**, *40*, 427−434. (q) Gupta, S. K.; Kuppuswamy, S.; Walsh, J. P. S.; McInnes, E. J. L.; Murugavel, R. *Dalton Trans.* **2015**, *44*, 5587−5601. (r) Gupta, S. K.; Dar, A. A.; Rajeshkumar, T.; Kuppuswamy, S.; Langley, S. K.; Murray, K. S.; Rajaraman, G.; Murugavel, R. *Dalton Trans.* **2015**,

44, 5961−5965. (s) Murugavel, R.; Walawalkar, M. G.; Pothiraja, R.; Rao, C. N. R.; Choudhury, A. *Chem. Rev.* **2008**, *108*, 3549−3655.

(11) Kalita, A. C.; Murugavel, R. *Inorg. Chem.* **2014**, *53*, 3345−3353.

(12) (a) Taylor, P. G.; Bassindale, A. R.; El Aziz, Y.; Pourny, M.; Stevenson, R.; Hursthouse, M. B.; Coles, S. J. *Dalton Trans.* **2012**, *41*, 2048−2059. (b) Chang, W.-K.; Wur, C.-S.; Wang, S.-L.; Chiang, R.-K. *Inorg. Chem.* **2006**, *45*, 6622−6627. (c) Kallus, S.; Patarin, J.; Marler, B. *Microporous Mater.* **1996**, *7*, 89−95. (d) Reinert, P.; Patarin, J.; Loiseau, T.; Ferey, G.; Kessler, H. *Microporous Mesoporous Mater.* **1998**, *22*, 43−45. (e) Matijasic, A.; Paillaud, J.-L.; Patarin, J. *J. Mater. Chem.* **2000**, *10*, 1345−1351. (f) Villaescusa, L. A.; Lightfoot, P.; Morris, R. E. *Chem. Commun.* **2002**, 2220−2221. (g) Taulelle, F.; Poblet, J. M.; Férey, G.; Bénard, M. *J. Am. Chem. Soc.* **2001**, *123*, 111−120.

(13) Kalita, A. C.; Gogoi, N.; Jangir, R.; Kuppuswamy, S.; Walawalkar, M. G.; Murugavel, R. *Inorg. Chem.* **2014**, *53*, 8959−8969.

(14) (a) Mahata, G.; Roy, S.; Biradha, K. *Chem. Commun.* **2011**, *47*, 6614−6616. (b) Biradha, K.; Domasevitch, K. V.; Moulton, B.; Seward, C.; Zaworotko, M. J. *Chem. Commun.* **1999**, 1327−1328. (b1) Roesky, H. W.; Andruh, M. *Coord. Chem. Rev.* **2003**, *236*, 91−119. (c) Pothiraja, R.; Sathiyendiran, M.; Butcher, R. J.; Murugavel, R. *Inorg. Chem.* **2005**, *44*, 6314−6323. (d) Pothiraja, R.; Sathiyendiran, M.; Butcher, R. J.; Murugavel, R. *Inorg. Chem.* **2004**, *43*, 7585−7587. (e) Rajakannu, P.; Howlader, R.; Kalita, A. Ch.; Butcher, R. J.; Murugavel, R. *Inorg. Chem. Front.* **2015**, *2*, 55−66.

(15) Bourne, S. A.; Moitsheki, L. J. *J. Chem. Crystallogr.* **2007**, *37*, 359−367. (b) Wang, D.-E.; Wang, F.; Meng, X.-G.; Ding, Y.; Wen, L.-L.; Li, D.-F.; Lan, S.-M. *Z. Anorg. Allg. Chem.* **2008**, *634*, 2643−2648. (c) Song, B.-Q.; Wang, X.-L.; Liang, J.; Zhang, T.; Shao, K.-Z.; Su, Z.-M. *CrystEngComm* **2014**, *16*, 9163−9167. (d) Baldoví, J. J.; Coronado, E.; Gaita-Ariño, A.; Gamer, C.; Giménez-Marqués, M.; Minguez Espallargas, G. *Chem. - Eur. J.* **2014**, *20*, 10695−10702. (e) Mistri, S.; Zangrando, E.; Figuerola, A.; Adhikary, A.; Konar, S.; Cano, J.; Manna, S. C. *Cryst. Growth Des.* **2014**, *14*, 3276−3285. (f) Liu, D.; Liu, X.; Liu, Y.; Yu, Y.; Chen, F.; Wang, C. *Dalton Trans.* **2014**, *43*, 15237−15244.

(16) (a) Hoffart, D. J.; Habermehl, N. C.; Loeb, S. J. *Dalton Trans.* **2007**, 2870−2875. (b) Aakeröy, C. B.; Epa, K. N.; Forbes, S.; Desper, J. *CrystEngComm* **2013**, *15*, 5946−5949. (c) Saraswatula, V. G.; Bhat, M. A.; Gurunathan, P. K.; Saha, B. K. *CrystEngComm* **2014**, *16*, 4715−4721. (d) Aakeröy, C. B.; Chopade, P. D.; Desper, J. *Cryst. Growth Des.* **2013**, *13*, 4145−4150.

(17) Dar, A. A.; Sharma, S. K.; Murugavel, R. *Inorg. Chem.* **2015**, *54*, 4882−4894.

(18) Andreev, V. P.; Vapirov, V. V.; Nizhnik, Y. P.; Aleshina, L. A.; Semenova, T. A. *Russ. J. Gen. Chem.* **2008**, *78*, 973−978.

(19) Gamoke, B.; Neff, D.; Simons, J. *J. Phys. Chem. A* **2009**, *113*, 5677−5684.

(20) (a) Flory, M. A.; McLamarrah, S. K.; Ziurys, L. M. *J. Chem. Phys.* **2006**, *125*, 194304−194311. (b) Shen, Q.; Hagen, K. *J. Phys. Chem.* **1987**, *91*, 1357−1360. (c) Gabe, E. J.; Le Page, Y.; Lee, F. L.; Barclay, L. R. C. *Acta Crystallogr., Sect. B: Struct. Crystallogr. Cryst. Chem.* **1981**, *37*, 197−200. (d) Brown, C. J.; Sadanaga, R. *Acta Crystallogr.* **1965**, *18*, 158−160.

(21) *Vogel's Text Book of Practical Organic Chemistry*, 5th ed.; Langman Group: Essex, Harlow, U.K., 1989.

(22) Dar, A. A.; Mallick, A.; Murugavel, R. *New J. Chem.* **2015**, *39*, 1186−1195.

(23) *WinGX*, version 1.64.05: Farrugia, L. J. *J. Appl. Crystallogr.* **1999**, *32*, 837−838.

(24) (a) Altomare, A.; Cascarano, G.; Giacovazzo, C.; Guagliardi, A.; Burla, M. C.; Polidori, G.; Camalli, M. *J. Appl. Crystallogr.* **1994**, *27*, 435−436. (b) Sheldrick, G. M. *Acta Crystallogr., Sect. A: Found. Crystallogr.* **2008**, *64*, 112−122.